Thessaloniki-GREECE 2007

4th International Conference on
Earthquake Geotechnical Engineering
June 25-28, 2007
Paper No. 1355

A NUMERICAL TOOL FOR THE DESIGN OF SLOPE STABILIZATION SYSTEMS USING RIGID INCLUSIONS

Ghazi HASSEN[1,2], Patrick de BUHAN[1], Alain PECKER[2]

ABSTRACT

A multiphase model is proposed for the elastoplastic analysis and design of slope stabilization systems based on the use of stiff linear inclusions, where shear and bending effects should be taken into account. A f.e.m-based numerical tool, incorporating a plasticity algorithm adapted to this multiphase model, is developed and illustrated on the example of a slope stabilized by such reinforcing inclusions. Emphasis is put in this analysis on the crucial role played by the shear and flexural behaviour of the inclusions in the slope stabilization.

Keywords: slope stability, reinforced soil; multiphase model; elastoplasticity; shear and bending effects.

INTRODUCTION

The use of reinforcing rigid inclusions, such as metal or concrete piles, in order to enhance the stability of soil structures, and more specifically to stabilize slopes in potentially unstable zones, is increasingly developed today. The strong heterogeneity of the composite reinforced soil, associated with the relatively high number of inclusions involved in such reinforcement techniques (up to several hundreds in some cases), makes it very difficult, if not impossible, to set up appropriate design oriented calculation methods, in which the inclusions could be treated as individual elements embedded in the native soil. Indeed, referring for instance to a finite element simulation of this kind of reinforced structure, and taking into account the cylindrical shape of the inclusions, a fully three dimensional analysis would be required, with a locally refined mesh discretization in order to capture with sufficient accuracy the rather complex interactions prevailing between the inclusions and the soil. This would inevitably lead to oversized numerical problems, or at least to the elaboration of a complex and sophisticated computational tool, the use of which would hardly be compatible with an engineering design.

In order to circumvent such difficulties, a new model, called “multiphase model”, has been recently proposed (de Buhan and Sudret, 2000), allowing to set up design methods for soil structures reinforced with linear inclusions, with a spectacularly reduced computational cost, compared to that required when trying to perform numerical simulations directly. For many applications, a simplified version of this model, where the reinforcement could be considered as “flexible”, that is working as axial load carrying structural elements (reinforced earth embankments or even soil nailed slopes and rock bolted tunnels), appears to be fully sufficient (Sudret and de Buhan, 2001). But, as concerns reinforcement techniques with rigid inclusions, such a simplification may be too conservative, in that it does not

[1] Ecole Nationale des Ponts et Chaussées, 6 et 8 av. B. Pascal, 77455, Marne-la-Vallée, cedex 02, France, Email : debuhan@lmsgc.enpc.fr
[2] Géodynamique et Structure, 157 rue des Blains, 92220, Bagneux, France, alain.pecker@geodynamique.com

account for the shear and flexural effects of the reinforcement, which could be expected to play a decisive role in some particular situations, and more importantly in slope stabilization systems. The main limitation of the simplified "multiphase model" may be overcome by developing a generalized model in which, referring to the beam-like characteristics of the reinforcement, their shear and flexural components, and not only their axial component, are incorporated in the analysis (Hassen and de Buhan, 2006). The objective of this contribution is to develop a first application of this model to the design of slope stabilization systems.

PROBLEM STATEMENT

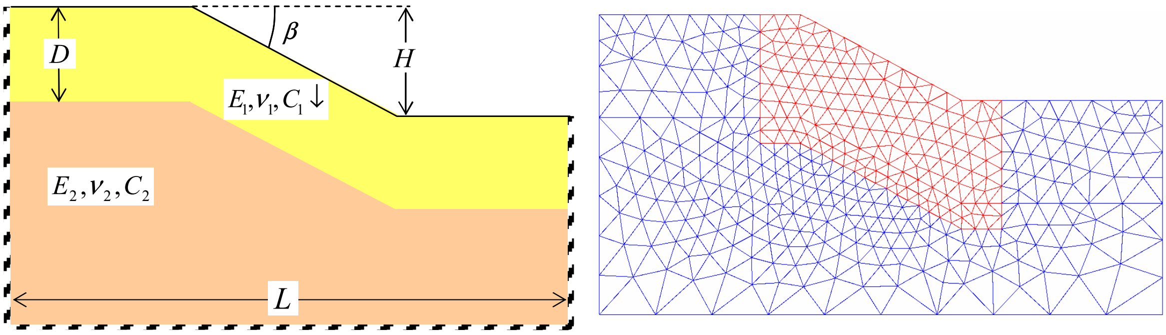

Figure 1. Finite element discretization of a two layer slope subject to its own weight

Figure 1 represents a slope of height H=10m and angle β with tanβ=1/2, subject to its own weight. It is formed by the superposition of a top layer of constant thickness D=12m, made of a soft soil lying upon a soil of much better characteristics. Both soils are assumed to be purely cohesive (clays), their mechanical behaviour being modelled through an elastic perfectly plastic constitutive law (Young's modulus E and cohesion C) with the following characteristics:

$$E_2 = 16\,\text{MPa}\,,\; \nu_2 = 0.3\;,\; C_2 = 80\,\text{kPa}\,,\; \gamma_2 = 25\text{kN/m}^3 \tag{1}$$

for the underlying soil, and

$$E_1 = 8\,\text{MPa}\,,\; \nu_1 = 0.3\;,\; C_1 = 40\text{kPa}\,,\; \gamma_1 = 20\text{kN/m}^3 \tag{2}$$

for the superficial soil layer.

Our objective is to evaluate the movements and the potential landslide generated by a sudden decrease of the superficial soil layer strength, triggered for instance by creep displacements, heavy rains, etc... The simulation is performed by applying the following procedure. Starting from an initial state where the slope is in equilibrium under its own weight, the strength (namely cohesion C_1) of the superficial soil is progressively (that is incrementally) reduced, thus producing plastic strains and related displacements leading to a new state of equilibrium. This step by step procedure, combined with a classical elastoplastic iterative algorithm, is carried out in the context of the finite element method. The right hand side in figure 1 displays the finite element mesh of the structure comprising 778 six-nodded triangular elements and 1615 nodes.

The results of the simulation are shown in figure 2 in the form of a curve giving the evolution of the displacement of a point located at the top of the slope as a function of the ratio between the soil reduced cohesion C_1^* and its initial value C_1. It can be seen that such a displacement tends to infinity as soon as this ratio drops below 80%, leading to the complete failure of the slope as illustrated in the right hand part of the same figure, where the corresponding failure mechanism entirely localized in the soft soil layer is represented.

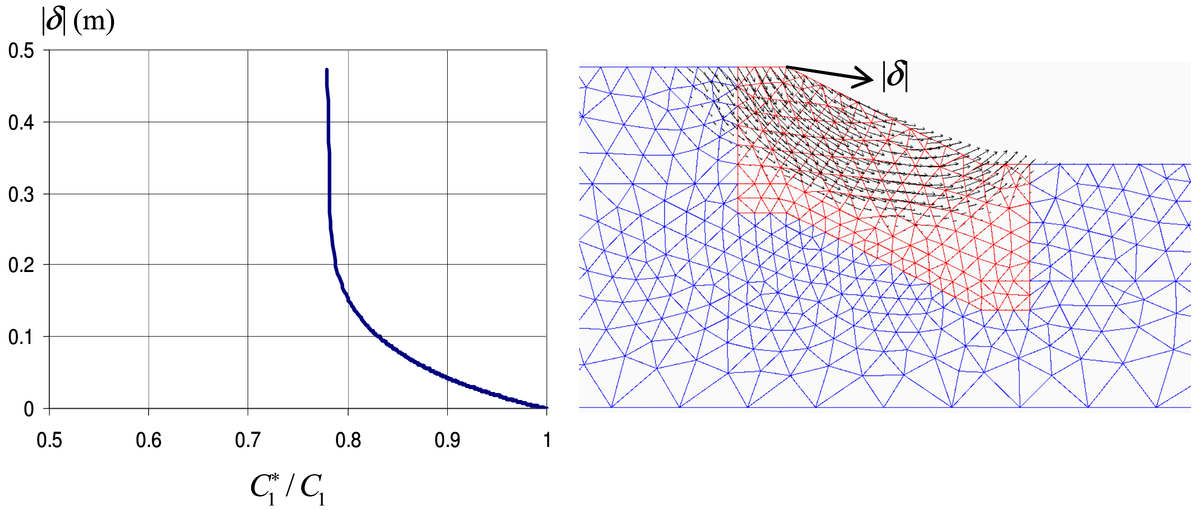

Figure 2. Displacements of the slope up to failure due to the soil strength reduction

In order to prevent such a failure, the slope has been reinforced in its central part by a group of vertical tubular steel piles of radius R=1m and thickness t=0.02m (figure 3). These reinforcing inclusions are placed into the soil mass at a regular square spacing s=5m. They are made of steel with the following mechanical characteristics:

$$E^s = 200\,\text{GPa}\,,\ \nu^s = 0.3\ ,\ \sigma_Y^s = 200\,\text{MPa} \tag{3}$$

where σ_Y^s denotes the steel tensile yield strength.

OUTLINE OF THE TWO-PHASE MODEL OF REINFORCED SOIL

According to the two-phase model advocated in this contribution, the composite reinforced soil is regarded as the superposition of two continuous media, called matrix and reinforcement phases, respectively. This notably means that matrix and reinforcement particles are geometrically coincident at any point, but may be attributed different kinematics. The matrix phase (which represents the soil) is endowed with the kinematics of a classical continuous medium, characterized at any point by a displacement vector $\underline{\xi}^m$, whereas the reinforcement phase (which represents the group of reinforcing piles) is modelled as a micropolar continuum, the kinematics of which is defined in each point by a displacement vector $\underline{\xi}^r$, along with a rotation $\omega^r \underline{e}_z$ (figure 3).

Equilibrium equations

Starting from this kinematic description, the virtual work method, and related principles, makes it possible to derive the set of equations governing the equilibrium of such a multiphase continuum (see

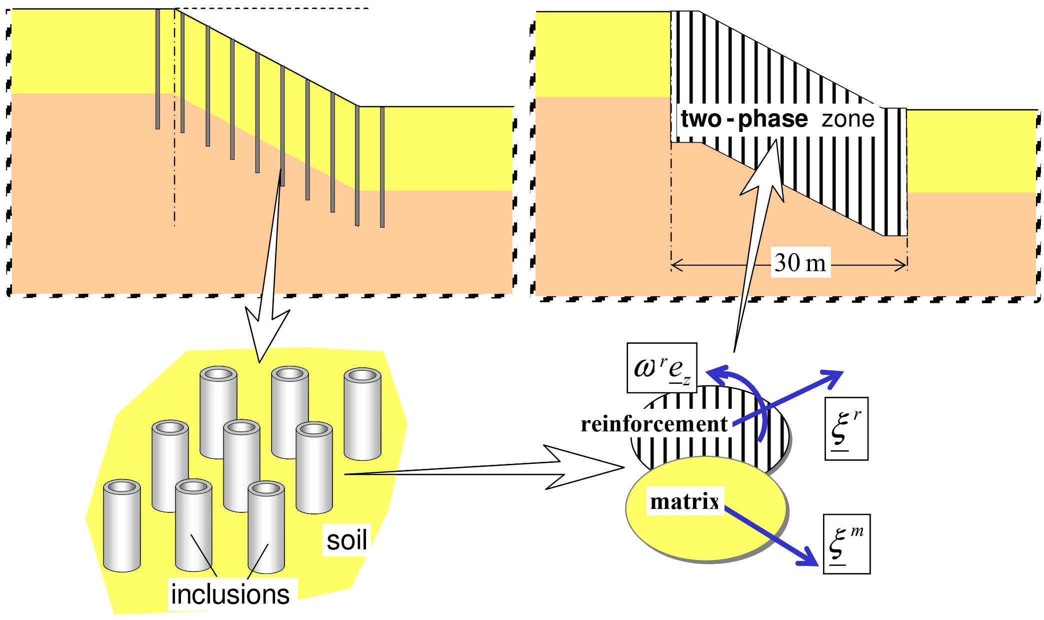

Figure 3. Slope stabilization by a group of vertical piles and principle of the two-phase model

de Buhan and Sudret (2000) or Hassen and de Buhan (2005, 2006) for more details). Those equations may be written as follows, for each phase separately:

$$\mathrm{div}\underline{\underline{\sigma}}^m + \rho^m \underline{F}^m + \underline{I} = 0 \tag{4}$$

for the matrix phase, and:

$$\frac{\partial(n^r \underline{e}_x + v^r \underline{e}_y)}{\partial x} + \rho^r \underline{F}^r - \underline{I} = 0 \quad , \quad \frac{\partial(m^r)}{\partial x} + v^r = 0 \tag{5}$$

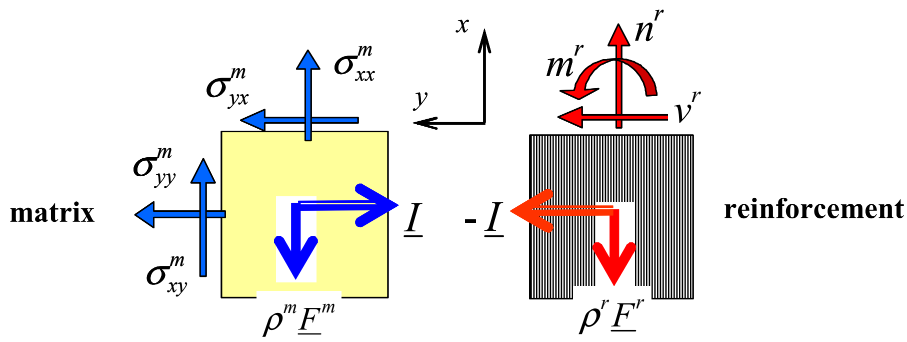

Figure 4. Stresses relative to the matrix and reinforcement phases

for the reinforcement phase, where $\underline{\underline{\sigma}}^m$ is the stress tensor defined at each point of the matrix phase, while n^r, v^r and m^r denote the densities of axial and shear forces, and bending moment, per unit transverse area to the reinforcement orientation. $\rho^m \underline{F}^m$ (resp. $\rho^r \underline{F}^r$) is the volume density of external body forces (such as gravity forces) applied to the matrix phase (resp. reinforcement phase), and finally $\underline{I}$ is the matrix-reinforcement interaction force volume density. Figure 4 illustrates the stresses involved in the two-phase description of a soil reinforced by rigid inclusions. The above equilibrium equations must be completed by stress boundary conditions prescribed for each phase separately.

Elastoplastic constitutive equations

In the context of small perturbations, the deformations in the matrix phase are classically described by the linearized strain tensor $\underline{\underline{\varepsilon}}^{m}$, while as regards the reinforcement phase, three strain variables, analogous to those encountered in the classical theory of one dimensional beams, are introduced, namely the axial strain ε^{r}, shear strain θ^{r} and curvature χ^{r}, defined as:

$$\varepsilon^{r}=\frac{\partial \xi_{x}^{r}}{\partial x}\ ,\ \ \theta^{r}=\frac{\partial \xi_{y}^{r}}{\partial x}-\omega^{r}\ \ ,\chi^{r}=\frac{\partial \omega^{r}}{\partial x} \tag{6}$$

Besides, the matrix-reinforcement interaction strain variable is:

$$\Delta\underline{\xi}=\underline{\xi}^{r}-\underline{\xi}^{m} \tag{7}$$

For the matrix phase the elastic perfectly plastic behaviour could be expressed by the classical constitutive law:

$$\underline{\underline{\sigma}}^{m}=\lambda^{m}\ \mathrm{tr}\left(\underline{\underline{\varepsilon}}^{m}-\underline{\underline{\varepsilon}}_{\mathrm{p}}^{m}\right)\underline{\underline{1}}+2\mu^{m}\left(\underline{\underline{\varepsilon}}^{m}-\underline{\underline{\varepsilon}}_{\mathrm{p}}^{m}\right) \tag{8}$$

where λ^{m} and μ^{m} are the Lamé coefficients and $\underline{\underline{\varepsilon}}^{m}{}_{\mathrm{p}}$ is the plastic strain tensor, the evolution of which is governed by a plastic flow rule:

$$\dot{\underline{\underline{\varepsilon}}}_{\mathrm{p}}^{m}=\dot{\eta}^{m}\frac{\partial g^{m}}{\partial \underline{\underline{\sigma}}^{m}}\ \ \text{with}\ \ \dot{\eta}^{m}=\begin{cases}\geq 0\ \text{ if }\ f(\underline{\underline{\sigma}}^{m})=\dot{f}(\underline{\underline{\sigma}}^{m})=0\\ =0\ \text{ otherwise}\end{cases} \tag{9}$$

where f^{m} is the yield function and g^{m} the plastic yield potential, these two functions being coincident in the case of an associated flow rule.

As concerns the reinforcement phase, the elastoplastic constitutive behaviour may be expressed in the form of three stress-strain scalar relationships:

$$n^{r}=\alpha^{r}(\varepsilon^{r}-\varepsilon_{\mathrm{p}}^{r})\ \ ,\ v^{r}=\beta^{r}(\theta^{r}-\theta_{\mathrm{p}}^{r})\ ,\ \ m^{r}=\gamma^{r}(\chi^{r}-\chi_{\mathrm{p}}^{r}) \tag{10}$$

where α^{r}, β^{r} and γ^{r} are the axial, shear and flexural stiffness densities of the reinforcement, per unit transverse area to the reinforcement orientation. The yield function, which defines the elastic domain, is formulated as a function of the three generalized stress components:

$$f^{r}(n^{r},v^{r},m^{r})\leq 0 \tag{11}$$

and the evolution of the plastic parts of the reinforcement-phase strain variables are expressed through the plastic flow rule:

$$\dot{\varepsilon}_{\mathrm{p}}^{r}=\dot{\eta}^{r}\frac{\partial f^{r}}{\partial n^{r}}\ ,\ \dot{\theta}_{\mathrm{p}}^{r}=\dot{\eta}^{r}\frac{\partial f^{r}}{\partial v^{r}}\ ,\ \dot{\chi}_{\mathrm{p}}^{r}=\dot{\eta}^{r}\frac{\partial f^{r}}{\partial m^{r}} \tag{12}$$

Likewise, the matrix-reinforcement interaction constitutive behaviour may be expressed as:

$$\underline{I}=\underline{\underline{c}}^{I}.\left[\Delta\underline{\xi}-\Delta\underline{\xi}_{\mathrm{p}}\right] \tag{13}$$

where $\underline{\underline{c}}^I$ is the interaction stiffness tensor and:

$$\Delta\dot{\underline{\xi}}_{\mathrm{p}} = \dot{\eta}^I \frac{\partial g^I}{\partial \underline{I}} \quad \text{with} \quad \dot{\eta}^I = \begin{cases} \geq 0 & \text{if} \quad f^I(\underline{I}) = \dot{f}^I(\underline{I}) = 0 \\ = 0 & \text{otherwise} \end{cases} \tag{14}$$

where, f^I (resp. g^I) is the yield criterion (resp. potential).

More details may be found in Hassen and de Buhan (2006) concerning the numerical treatment of these constitutive equations, and their implementation in a finite element code.

APPLICATION TO THE DESIGN OF THE SLOPE STABILIZATION SYSTEM

According to the two-phase model advocated in this contribution, the composite reinforced soil zone is replaced by a two-phase homogeneous zone, shown in figure 3. The major advantage of this model lies in the fact that, unlike in the case of a direct implementation of the finite element method to the simulation of the reinforced slope, which would have required a highly refined discretization of the structure, the same finite element mesh as that used for the non reinforced slope (figure 1) can be employed. It should be emphasized in particular that the typical size of the mesh elements in the reinforced zone is in no way different from that adopted in the absence of reinforcement and no remeshing procedure is required when the different characteristics of the reinforcement (spacing, diameter, thickness, etc.) are modified.

Determination of input model parameters

The elastic as well as yield parameters of the two-phase components to be introduced in the numerical simulations may then be determined as follows. It is first to be noted that, in the reinforced zone, the reinforcement volume fraction can be easily calculated as the ratio between the cross-sectional area of one individual pile and the total cross section s^2 of the representative volume of reinforced soil, namely:

$$\eta = \frac{2\pi R t}{s^2} \cong 0.5\% \tag{15}$$

so that the soil volume fraction, equal to 1-η is close to unity. Therefore, it seems reasonable to adopt for the matrix phase in the reinforced zone, the same elastic and plastic characteristics as for the corresponding upper soil layer.

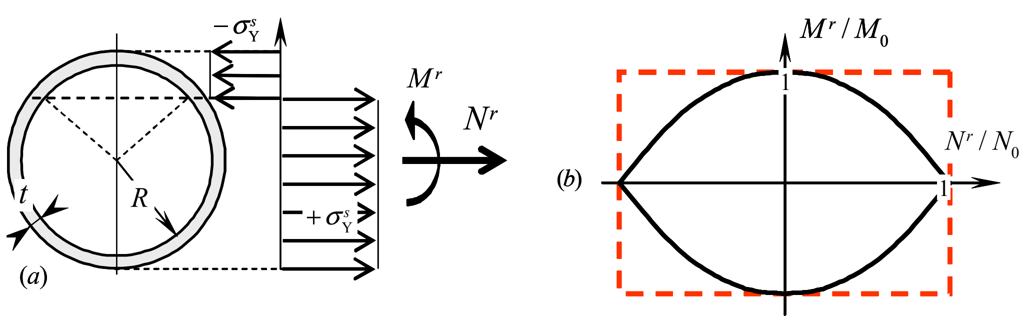

Figure 5. Interaction diagram for an individual reinforcing pile

As regards the reinforcement phase, the axial, shear and bending stiffness densities are simply calculated, by dividing the corresponding quantities relative to one individual reinforcing inclusion by the area s^2 of the representative volume's cross section. One obtains from this straightforward procedure:

$$\alpha^r = \frac{AE^s}{s^2} = 1004 \text{ MPa} \ , \ \beta^r = \frac{A^* \mu^s}{s^2} = 193 \text{ MPa} \ , \ \gamma^r = \frac{IE^s}{s^2} = 502 \text{ MPa.m}^2 \tag{16}$$

where $A=2\pi Rt$ is the inclusion cross section, $A^*=A/2$ its shear cross section (see for instance Frey (1994)), $I=\pi R^3 t$ its bending moment and μ^s the steel shear modulus.

Likewise, the reinforcement phase yield strength properties, expressed by means of a criterion such as (11), may be determined from the solution to a yield design problem, sketched in figure 5, in which a section of pile is submitted to the combination of an axial force N^r and bending moment M^r. Exploring uniaxial stress distributions in the pile cross-section, as that sketched in figure 5, allows to derive the following interaction formula for a single tubular pile (Challamel and de Buhan, 2003):

$$\left|\frac{M^r}{M_0}\right| - \cos\left(\frac{\pi}{2}\frac{N^r}{N_0}\right) \leq 0 \quad \text{with} \quad \begin{cases} N_0 = 2\pi Rt\sigma_Y^s \\ M_0 = 4R^2 t\sigma_Y^s \end{cases} \tag{17}$$

This interaction formula, which is represented in figure 5 (solid line), implicitly assumes that the pile is infinitely resistant to shear forces. It follows that the reinforcement phase yield strength condition (10) writes:

$$f^r(n^r, m^r) = \left|\frac{m^r}{m_0}\right| - \cos\left(\frac{\pi}{2}\frac{n^r}{n_0}\right) \leq 0 \quad \text{with} \begin{cases} n_0 = 2\pi Rt\sigma_Y^s / s^2 = \eta\sigma_Y^s \cong 1\text{MPa} \\ m_0 = 4R^2 t\sigma_Y^s / s^2 = \dfrac{2}{\pi}\eta R\sigma_Y^s \cong 0.64\text{MPa.m} \end{cases} \tag{18}$$

which, for the sake of simplicity in the subsequent elastoplastic calculations, will be approximated by the following upper bound condition (dashed rectangle in figure 5):

$$|n^r / n_0| \leq 1 \ , \ |m^r / m_0| \leq 1 \tag{19}$$

Results of numerical simulations

The consequence of reinforcement on the slope stabilization is clearly apparent in figure 6, which displays the same kind of curve as that already drawn in figure 2 for the unreinforced slope. For instance, for a residual strength of the superficial layer equal to 40% of the initial one, the movements of the slope remain limited since the displacement at the top of the slope is less than 0.15m. Complete instability of the reinforced slope occurs when the superficial soil cohesion is reduced by 80%. The associated failure mechanism involves a much larger zone than in the case of the unreinforced slope.

CONCLUSION

The elastoplastic two phase model described in this contribution and developed in the form of a f.e.m-based numerical code, allows for the simulation and design of any reinforced soil structure, leading to a spectacular reduction of the computational cost, as soon as a relatively great number of reinforcing inclusions is concerned. Its potential effectiveness has been demonstrated on an example of a slope becoming gradually unstable due to degradation of its strength characteristics and that can be stabilized with stiff steel piles as long as the original soil strength does drop below a certain percentage of its original value.

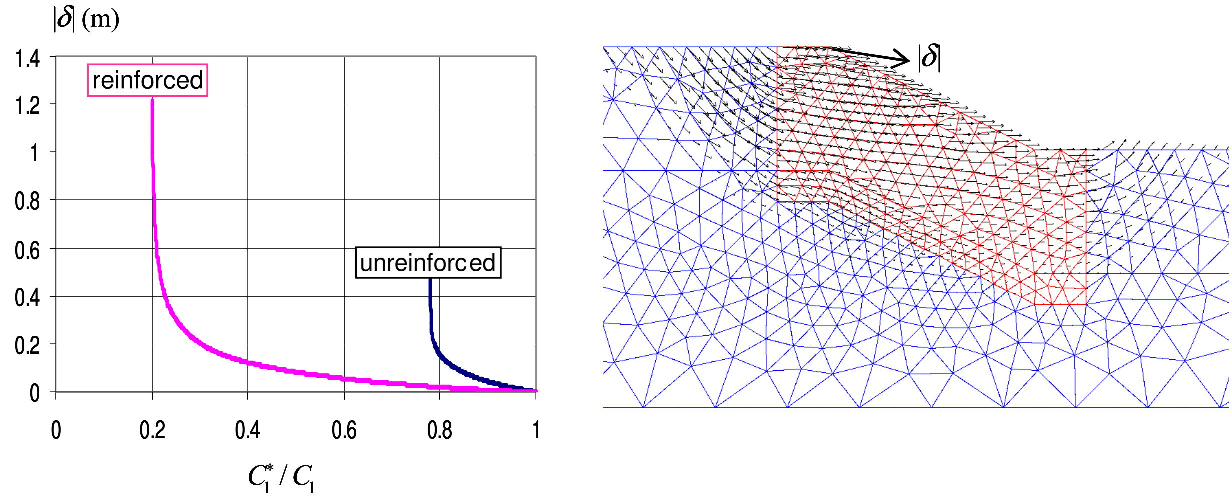

Figure 6. Effect of reinforcement on the slope stabilization

ACKNOWLEDGEMENTS

The work presented in this contribution has been financially supported by the European Union in the framework of the LESSLOSS project under contract GOCE-CT-2003-505448.

REFERENCES

de Buhan P., Sudret B. (2000). Micropolar multiphase model for materials reinforced by linear inclusions. *Eur. J. Mech. A/Solids* 19, p. 669-687

Sudret B., de Buhan P. (2001). Multiphase model for inclusion-reinforced geostructures. Application to rock-bolted tunnels and piled raft foundations. *Int J Num Anal Meth Geomech*, 2001; 25:155-182.

Hassen G., de Buhan P. (2006). Elastoplastic multiphase model for simulating the response of piled raft foundations subject to combined loadings. *Int J Num Anal Meth Geomech*, 2006; 30:843-864.

Hassen G., de Buhan P. (2005). A two-phase model and related numerical tool for the design of soil structures reinforced by stiff linear inclusions. *Eur. J. Mech. A/Solids* 24, p. 987-1001

Challamel N., de Buhan P. (2003). Mixed modelling applied to soil-pipe interaction. *Comp. and Geotech.*, 30, pp. 205-216.

Frey F. (1994). *Analyse des structures et milieux continus*. Vol. 2, Presses Polytechniques et Universitaires Romandes.